SMC-TR-94-21

AEROSPACE REPORT NO.
TR-92(2935)-11

(1)

Surface Contamination on LDEF Exposed Materials

15 June 1992

Prepared by

C. S. HEMMINGER
Mechanics and Materials Technology Center
Technology Operations

Prepared for

SPACE AND MISSILE SYSTEMS CENTER
AIR FORCE MATERIEL COMMAND
2430 E. El Segundo Boulevard
Los Angeles Air Force Base, CA 90245

Engineering and Technology Group

THE AEROSPACE
CORPORATION

This report was submitted by The Aerospace Corporation, El Segundo, CA 90245-4691, under Contract No. F04701-88-C-0089 with the Space and Missile Systems Center, 2430 E. El Segundo Blvd., Los Angeles Air Force Base, CA 90245. It was reviewed and approved for The Aerospace Corporation by S. Feuerstein, Principal Director, Mechanics and Materials Technology Center.

This report has been reviewed by the Public Affairs Office (PAS) and is releasable to the National Technical Information Service (NTIS). At NTIS, it will be available to the general public, including foreign nationals.

This technical report has been reviewed and is approved for publication. Publication of this report does not constitute Air Force approval of the report's findings or conclusions. It is published only for the exchange and stimulation of ideas.

10 FEB 94

Wm. Kyle Snedden, Captain USAF
Deputy, Industrial & International Division

REPORT DOCUMENTATION PAGE

Form Approved OMB No. 0704-0188

1. AGENCY USE ONLY (*Leave blank*)	2. REPORT DATE	3. REPORT TYPE AND DATES COVERED
	15 June 1992	

4. TITLE AND SUBTITLE
Surface Contamination on LDEF Exposed Materials

5. FUNDING NUMBERS
F04701-88-C-0089

6. AUTHOR(S)
Hemminger, Carol S.

7. PERFORMING ORGANIZATION NAME(S) AND ADDRESS(ES)
The Aerospace Corporation
Technology Operations
El Segundo, CA 90245-4691

8. PERFORMING ORGANIZATION REPORT NUMBER
TR-92(2935)-11

9. SPONSORING/MONITORING AGENCY NAME(S) AND ADDRESS(ES)
Space and Missile Systems Center
Air Force Materiel Command
2430 E. El Segundo Boulevard
Los Angeles Air Force Base, CA 90245

10. SPONSORING/MONITORING AGENCY REPORT NUMBER
SMC-TR-94-21

11. SUPPLEMENTARY NOTES

12a. DISTRIBUTION/AVAILABILITY STATEMENT
Approved for public release; distribution unlimited

12b. DISTRIBUTION CODE

13. ABSTRACT (*Maximum 200 words*)

X-ray photoelectron spectroscopy (XPS) has been used to study the surface composition and chemistry of Long Duration Exposure Facility (LDEF) exposed materials. In each set of samples, silicones were the major contributors to the molecular film accumulated on the LDEF exposed surfaces. All surfaces analyzed have been contaminated with Si, O, and C; most have low levels (<1 atom%) of N, S, and F. The contaminant overlayer is thought to be patchy, with significant areas covered by less than 100 Å of molecular film. For most materials analyzed, Si contamination levels were higher on the leading-edge surfaces than on the trailing-edge surfaces. It is probable that the return flux associated with atmospheric backscatter resulted in enhanced deposition of silicones and other contaminants on the leading-edge flight surfaces relative to the trailing edge. XPS analyses, however, did not conclusively show different relative total thicknesses of flight-deposited contamination for leading- and trailing-edge surfaces. Unlike other materials, exposed polymers, such as Kapton and FEP-type Teflon, had very low contamination on the leading-edge surfaces. SEM evidence showed that undercutting of the contaminant overlayer and damaged polymer layers occurred during atomic oxygen erosion, which would enhance loss of material from the exposed surface.

14. SUBJECT TERMS
LDEF, Contamination, XPS

15. NUMBER OF PAGES
25

16. PRICE CODE

17. SECURITY CLASSIFICATION OF REPORT	18. SECURITY CLASSIFICATION OF THIS PAGE	19. SECURITY CLASSIFICATION OF ABSTRACT	20. LIMITATION OF ABSTRACT
UNCLASSIFIED	UNCLASSIFIED	UNCLASSIFIED	

PREFACE

The author would like to acknowledge the many contributors to this work within The Aerospace Corporation, including T. Giants, S. Gyetvay, C. Jaggers, T. Le, J. Mallon, N. Marquez, M. Meshishnek, G. Radhakrishnan, G. Steckel, W. Stuckey, C. Su, and J. Uht. In addition, I would like to thank H. G. Pippin of Boeing Aerospace & Electronics, W. Slemp of NASA Langley Research Center, E. Lan of McDonnell Douglas Astronautics Company, and D. Wallace of QCM Research for making samples available to us. I also thank D. Wheeler of NASA Lewis Research Center for his helpful discussions on Teflon radiation damage.

CONTENTS

FIGURES

TABLES

I. INTRODUCTION

In the course of LDEF post-retrieval investigations, XPS has been used to study the surface composition and chemistry of exposed materials, including Ag/FEP, Kapton, S13GLO paint, QCMs, carbon fiber/organic matrix composites, and carbon fiber/Al alloy composites. One objective of this study was to compare typical surface contamination types and coverages on leading and trailing edge LDEF exposed surfaces for a variety of materials. Analysis of anomalies and other "nonrepresentative" areas was generally avoided in an attempt to maximize data acquisition for areas with average exposure to the space environment. XPS is an excellent surface analysis technique for the study of contaminant overlayers. Each XPS analysis provides an average semi-quantitative surface composition over an area approximately 4 x 5 mm, with an analysis depth of 50 to 100 Å. All elements can be detected except hydrogen and helium. The details of electron energies and peak shapes give information about the chemical state of many elements in the sample surface. Minimal sample preparation of LDEF exposed materials was required for XPS analysis, and the analysis was nondestructive unless the surface components were radiation sensitive. Surface charging of insulators and semiconductors does not pose a major problem for the XPS technique, allowing straightforward analysis of surface oxides and contamination layers. Complementary SEM/EDS analysis was used to look at many of the same samples. EDS analysis provides an average semi-quantitative surface composition over the area rastered by the electron beam, with an analysis depth of ≤ 1 μm.

II. EXPERIMENTAL

The LDEF exposed materials and their reference samples investigated in this study are listed in Table 1. The LDEF experiment and exposure position of the samples is included in the table, where the notation "D9" indicates bay D/row 9 of LDEF. Some materials were analyzed with no sample preparation other than mounting on an appropriate sample stub. Most, as indicated in Table 1, were cut to provide samples that could be introduced into the analysis system. Additional information about the materials is given in Table 2.

The LDEF exposed and reference samples were analyzed by XPS using a VG Scientific LTD ESCALAB MK II instrument. The samples were mounted on sample stubs with strips of tantalum foil or with double-sided tape. Survey scans from 0 to 1100 eV binding energy were acquired to qualitatively determine the sample surface composition. Analysis areas were about 4 x 5 mm in size and analysis depth was about 50 to 100 Å. Data acquisition with a Mg Kα and an Al Kα source was used to check for all the elements of interest. High resolution elemental scans were subsequently run to obtain semi-quantitative elemental analyses from peak area measurements and chemical state information from the details of binding energy and shape. Measured peak areas for all detected elements were corrected by elemental sensitivity factors before normalization to give surface mole %. The quantitation error on a relative basis is $\leq$10% of the measurement for components with a surface concentration >1 mole %. Large uncertainties in the relative elemental sensitivity factors can introduce absolute errors of a factor of 2 or even greater. The detection limit is about 0.1 surface mole %, but spectral overlaps between large peaks and small peaks can make it impossible to detect minor components, particularly when more than one chemical state is present for a given element.

A JEOL 840 SEM with an EDAX 9900 EDS system was used for the SEM/EDS analyses. Nonconductive surfaces were coated by carbon evaporation to minimize surface charging effects.

Table 1. LDEF Exposed Material and Reference Samples Investigated

LDEF exposed material	Experiment and location	Sample preparation	Reference samples
Carbon fiber/Al alloy composite	M0003; D8 and D4	1/2 inch squares cut	Flight controls Laboratory controls
Carbon fiber/organic matrix composites	M0003; D9 and D3	1/2 inch squares cut	Backside flight controls
S13GLO paint	M0003; D9 and D3	As-received	Laboratory reference
Quartz crystals from QCMs	M0003; D9 and D3	Crystals dismounted from QCMs and acetone-washed at QCM Research	Reference QCM crystals
Kapton	A0076; F9	1/2 inch square cut	Laboratory reference
Ag/FEP, thermal control blankets	A0004-1; F2 A0178; D1, A2, A4, F4, B5, C5, D5, C6, B7, D7, C8, A10, C11, D11	1/2 inch squares cut	Laboratory controls Masked edge flight controls
Ag/FEP, adhesively mounted thermal control sheets	M0003; D9 A0076; F9	1/2 inch squares cut	Laboratory references Masked edge flight controls

Table 2. LDEF Exposed Material Information

LDEF exposed material	Supplier	Additional information
Carbon fiber/Al alloy composite	Fiber Materials, Inc.	GY70 graphite fibers, manufactured by BASF Structural Materials Inc., reinforcing Al alloy 201 matrix with 2024 Al alloy surface foils. Major components of 2024 alloy are 93% Al, 4.4% Cu, 1.5% Mg and 0.6% Mn.
Carbon fiber/organic matrix composites	The Aerospace Corporation	T300 woven fabric, manufactured by Amoco Performance Products, Inc., reinforcing poly(arylacetylene) materials that were under development at The Aerospace Corporation in 1984.
S13GLO paint	I. I. T. Research Institute; coupons made by TRW	White thermal control paint. Zinc oxide pigment encapsulated in potassium silicate with a methyl silicone binder.
Quartz crystals from QCMs	QCM Research	Active QCMs used crystals with 9000Å Al + Al_2O_3 plus 150 Å In_2O_3 top layer. The top layer on passive QCMs was 150Å ZnS.
Kapton	E. I du Pont de Nemours & Co., Inc.	A polyimide.
Ag/FEP, thermal control blankets	Sheldahl	5 mil FEP Teflon, manufactured by E. I du Pont de Nemours & Co., Inc.
Ag/FEP, adhesively mounted thermal control sheets	Sheldahl	2 mil FEP Teflon, manufactured by E. I du Pont de Nemours & Co., Inc.

III. RESULTS AND DISCUSSION

A. CONTAMINATION ON COMPOSITE, PAINT, AND QCM SURFACES

The XPS data for the carbon fiber/Al alloy composite samples are shown in Table 3. The entire XPS signal should come from the 2024 Al alloy surface foil, which was shown to be intact by SEM, and its contamination overlayer. The flight surfaces had visible discoloration. The exposed side of the trailing edge sample had a pale brown stain. The exposed side of the leading edge sample had a rainbow-like light dispersion in some areas, and its backside had a very pale brown stain. The laboratory and flight control surfaces did not have visible discoloration. The flight control sample had been mounted on the backside of the D4 cassette.

The laboratory control surfaces were contaminated with C, Si, N, Na, K, Ca, F, Cl, P, and S. Pre-launch contamination was clearly significant. This points out how laboratory control samples can be critical to the assessment of on-flight contamination and material modification. The flight control surfaces and sample backsides (another commonly used "flight control") had higher concentrations of Si contamination than the lab control surfaces by more than a factor of 2. The observed variability for Si (7 to 28%) on these four surfaces was a factor of 4, showing the inherent inaccuracy of using only flight controls for comparison to the exposed surfaces. The contamination on the leading edge sample backside surface was particularly high, possibly due to preflight or postflight contamination. The Si concentration on the exposed surfaces was a factor of 2 higher than on the flight controls. Si contamination was about 25% higher on the leading edge exposed surface than on the trailing edge exposed surface. Si was detected predominantly as SiO_2 on both exposed flight surfaces and on the leading edge sample backside; this assignment was based on a Si2p binding energy of 103.5 ± 0.2 eV after charge correction. On the other surfaces, the Si2p peak was detected at lower binding energy, 102.9 + 0.3 eV, which indicated surface silicone or possibly mixed silicone/silicate/silica. It was not possible to determine the source of carbon on the flight surfaces: it could come from silicone and/or hydrocarbon deposition and/or from the preflight contaminant overlayer.

Table 3. XPS Data for Carbon Fiber/Aliminum Alloy Composites

		Surface Mole %, Normalized														
Sample		Al	Mg	O	Si	C	Na	K	Ca	F	Cl	P	S	N	Sn	Cu
AL3-3, Leading Edge	Exposed	0.4	nds	65	29	6	tr	tr	nds	nds	tr	nds	nd	nd	nds	nds
	Backside	0.2	nd	65	28	4	2	nd	tr	tr	tr	nd	0.2	0.1	tr	tr
AL5-11, Trailing Edge	Exposed	0.7	nds	59	23	13	3	0.1	nds	0.3	0.2	nds	0.2	0.4	0.1	nds
	Backside	11	2	51	7	20	3	0.7	0.3	0.8	0.3	0.5	2	1	0.2	0.1
AL5-13, Flight Control	Side 1	5	0.8	43	11	37	0.7	0.2	0.3	0.6	0.4	0.2	0.3	1	0.2	tr
	Side 2	3	0.5	41	11	40	1	0.3	0.2	0.3	0.4	0.1	0.3	2	0.2	tr
AL3-14, Lab Control	Side 1	9	0.8	35	2	49	1	0.2	0.3	0.1	0.3	tr	0.4	2	nd	nds
	Side 2	8	1	35	3	49	1	0.2	0.3	0.1	0.2	0.3	0.3	2	nd	nds

tr = trace (<0.1)
nd = not detected
nds = not detected survey scan; no high resolution scan run

Aluminum was detected as the oxide, Al_2O_3, on all sample surfaces, as would be expected for air-exposed alloy. It is possible that postflight air oxidation could mask on-flight changes. Only the predominant chemical state of the alloy surface could be detected in the presence of the contaminant overlayer. The weak Al signal (<1%) on the exposed flight surfaces implies a contaminant coverage at least comparable to the depth probed by XPS, 50 to 100 Å. In the case of noncontinuous or nonuniform coverage, the average thickness of the contaminant overlayer could be substantially greater. Stronger Al signals (3 to 11%) on the control and trailing edge backside surfaces indicate relatively lower contaminant thickness/coverage.

The XPS data for the carbon fiber/organic matrix composites are shown in Table 4. The composites were designated as A, B, and C, and had been fabricated with differences in the matrix. The "L" and "T" prefixes in Table 4 indicates leading and trailing edge, respectively. No laboratory control samples were available for these samples, and the sample backsides were used as the flight controls. These carbon/poly (arylacetylene) (PAA) materials were under development at The Aerospace Corporation in 1984 as replacements for more traditional composites such as carbon/epoxy. The exposed leading edge surfaces were visibly eroded. SEM and optical microscopy showed the erosion to be irregular to a depth of about 5 mils.[1] The erosion morphology was dominated by crevasses parallel to the fibers, with triangular cross sections. The edges of the crevasses were well-defined, and penetrated through both matrix and fibers. The exposed trailing edge samples and sample backsides exhibited no physical appearance changes due to exposure.

Table 4. XPS Data for LDEF Fiber/Organic Matrix Composites

			Surface Mole %, Normalized												
		Imaged?	C	O	Si	N	F	S	Cl	Cu	Zn	Ni	Sn	Na	P
L-A	Exposed	Yes	45	42	10	2		0.6		0.3					
	Exposed	No	44	44	8	1	0.4	0.5	tr	2	0.3				
	Backside	No	71	20	2	2	3	0.1	0.1	1	tr				
T-A	Exposed	No	51	36	6	2	3	tr	0.1	3	0.2		0.1		
	Backside	No	66	26	2	1	3	0.2	0.1	1					
L-B	Exposed	Yes	17	59	19	0.6	nd	0.3	0.1	2	tr	1		nd	0.3
	Backside	Yes	59	31	3	2	2	0.2	0.2	2	nd			1	nd
T-B	Exposed	Yes	45	23	4	0.9	25	0.1	0.1	1	0.1			0.1	
	Exposed	No	46	27	3	1	19	0.1	0.2	2	0.2			1	
	Backside	Yes	70	22	2	1	3	0.1	0.2	0.7	nd			0.2	nd
L-C	Exposed	Yes	61	31	3	3	0.1	0.5	nd	0.3	nd		0.4	0.3	0.6
	Backside	Yes	67	23	4	2	3	0.1	0.2	2	nd		nd	0.1	nd
T-C	Exposed	Yes	47	39	7	2	0.4	0.2	0.4	5	0.4		tr	0.1	nd
	Backside	Yes	65	24	4	1	0.3	nd	0.3	1	0.2		tr	nd	nd
Release Cloth		No	39	4	0.7		56								

tr = trace
nd = not detected in elemental scan
blank = not detected in survey scan and no elemental scan acquired

Comparison of Si concentration on leading and trailing edge surfaces showed a much broader range of values on the leading edge: 3 to 19% Si on the leading vs. 4 to 7% on the trailing edge. A comparison of the Si concentration on pairs of leading and trailing edge composites gave the widely varied ratios of 1.7, 4.8, and 0.4. Si contamination was highest on sample L-B, which had lower erosion than L-A and L-C. Composite B had the lowest resin content of the three: 22% by weight compared to 37% and 33% for composites A and C, respectively. It is unknown if the surface contamination plays a role in erosion crevasse initiation and enlargement. Si concentration on the sample backsides ranged from 2 to 4%. Si ratios for exposed leading edge surfaces to their backsides were 5.0, 6.3, and 0.8. Si ratios for exposed trailing edge surfaces to their backsides were 3.0, 2.0, and 1.8. The predominant chemical state of Si detected was SiO_2 on all of the exposed surfaces, both leading and trailing edges. The Si detected on the samples backsides was predominantly from silicone or mixed silicone/silicate/ silica. The lack of laboratory controls prevents conclusions about changes in the composite surface chemistry and about the wide range of minor contaminants, including N, F, S, Cl, Cu, Zn, Ni, Sn, Na, and P. One surface had 25% F; release cloth used in fabrication is the most likely source of fluorocarbon contamination. It is likely that preflight contamination is significant as a source of minor contaminants.

The XPS data for S13GLO paint are shown in Table 5. There were no flight control or backside surfaces, nor were laboratory controls maintained. A laboratory reference was prepared for comparison from a current batch of S13GLO. Visible changes were seen in the flight surfaces. The trailing edge surfaces had brown discoloration, with some lighter lines and spots. Little discoloration was observed on the leading edge surfaces. Interpretation of surface contamination was complicated because the binder is methyl silicone, and by the lack of a same-batch laboratory control. On all flight exposed surfaces, the C signal decreased and the O signal increased, relative to Si. The Si2p binding energy and O to Si concentration ratio changed from silicone to SiO_2 on leading and trailing edge surfaces. Exposure to UV radiation and atomic oxygen in the space environment caused silicone degradation, with resulting formation of SiO_2 and loss of carbon through volatiles. This investigation was inconclusive on the question of silicone binder decomposition vs. silicone contaminants deposition/decomposition as the source of measured surface Si. It was observed that the leading edge surfaces had greater loss of carbon than trailing edge surfaces. The SEM analysis was inconclusive on whether a significant amount of binder was lost from leading edge surfaces due to atomic oxygen erosion. K and Zn from the pigment was detected on all flight samples, but not on the reference. This may indicate some binder loss, but it may also be due to a difference between batches of S13GLO.

Table 5. XPS Data for S13GLO Paint

		Surface Mole % (Normalized)									
S13GLO Paint Sample		C	O	Si	K	Zn	N	S	Cl	Na	F
	Reference	44	30	26	0.2	nd	nd	nd	nd	nd	nd
L31V-18-17-1	Leading	12	56	27	1	0.5	2	0.3	0.5	0.3	0.1
L31V-18-18-2	Leading	13	56	27	1	0.5	2	0.2	0.5	0.3	0.1
T31V-18-17	Trailing	28	46	21	0.8	0.3	2	0.4	0.4	0.7	0.5
T31V-18-18	Trailing	27	47	21	1	0.2	2	0.4	0.4	0.8	0.4

The XPS data for the QCM crystals are shown in Table 6. The reference crystals served as flight control samples for the sense crystals. Laboratory control samples have not been made available. The flight surfaces were not visibly altered by space environment exposure. The QCMs were disassembled at QCM research and all the crystals were cleaned in acetone at that time, before delivery to The Aerospace Corporation for analysis. Solvent washing can remove some surface contaminants and leave new residues. It is possible that these residues explain the observation that most of the crystal surfaces were contaminated with $\geq$ 50% carbon. SEM/EDS analysis showed the thin 150Å top layers to still be present on all the crystals. Thus, the low signals for In, Zn, and Al, < 1.5% for all crystal surfaces, indicate average contamination coverage comparable to the depth of analysis. Si contamination was detected on all but one surface, a reference crystal. The Si surface contamination was higher on the leading edge surfaces relative to the trailing edge surfaces for both sense and reference crystals, but was highest for the leading edge sense crystals at 10 and 23%. The Si concentration leading edge/trailing edge ratio for the flight exposed sense crystals was 4 for the passive QCMs and 15 for the active QCMs. The predominant Si species on both leading edge exposed surfaces was SiO_2. On all other crystal surfaces, Si was detected as silicone or a mix of silicone/silicate/silica. Some of the surface contamination observed on the crystal surfaces may be due to other components of the QCMs, such as Sn and Pb from solder, or N and Ag from conductive epoxy.

Table 6. XPS Data for QCM Contamination Monitors

				Surface Mole %, Normalized												
QCM		Crystal	Top Layer	C	O	Si	In	Sn	Zn	S	Pb	K	Na	N	Cl	Al	Ag
TP 329, Active	1	Sense	In_2O_3	17	58	23	0.7	0.2	nd	0.1	nd	tr	0.3	0.8	tr	nd	nd
Leading Edge	2	Reference	In_2O_3	53	31	1.9	6.4	1.0	0.1	0.1	0.5	0.1	1.0	4.5	0.2	nd	nd
TP 330, Passive	3	Sense	ZnS	48	35	10	nd	0.2	0.9	0.5	0.1	tr	0.4	3.5	0.1	1.4	nd
Leading Edge	4	Reference	ZnS	61	23	1.0	nd	0.2	2.0	5.5	0.3	tr	0.7	4.7	0.4	nd	1.2
TP 318, Active	5	Sense	In_2O_3	68	25	1.5	nd	0.3	nd	0.1	0.3	nd	0.1	4.7	0.2	0.4	nd
Trailing Edge	6	Reference	In_2O_3	65	24	0.2	2.3	0.7	0.1	0.2	0.4	nd	0.1	6.3	0.1	nd	nd
TP 353, Passive	7	Sense	ZnS	67	25	2.3	nd	0.4	0.1	0.1	0.4	nd	0.1	4.5	0.3	nd	nd
Trailing Edge	8	Reference	ZnS	68	20	nd	nd	0.3	1.4	3.9	0.3	tr	0.3	4.1	0.3	nd	0.6

tr = trace (< 0.1)
nd = not detected

1. Conclusions

An overview of the XPS analyses of LDEF exposed composite, paint, and QCM crystal surfaces shows their surface contamination to be nonuniform and complex. Interpretation of the data is hindered by the uncertainty of preflight and postflight contaminants, and by the lack of comparable laboratory and flight controls for each type of material. However, the following observations are consistent for all of these samples. Silicones were a major contributor to the accumulated molecular film. The predominant surface

species of Si was identified as SiO_2 on almost all of the exposed flight surfaces, and as silicone or a mix of silicone/silicate/silica on flight controls including backside surfaces. It is thought that UV and atomic oxygen exposure causes decomposition of surface-deposited silicones, with SiO_2 as one of the products. For most pairs of samples, the Si contamination level was higher on the leading edge surface than on the trailing edge surface. Measured Si concentration leading edge/trailing edge ratios varied from 0.4 to 15, with a median of about 1.5 and an average of about 4. Atmospheric backscatter could play a major role in enhancing non-line-of-sight deposition of outgassed species onto the leading edge exposed surfaces.

It was not possible to use the XPS data to distinguish hydrocarbons or other organic species deposited during flight from the preflight, postflight, and substrate sources of surface carbon. The relative surface carbon concentration is generally higher on the trailing edge exposed surfaces than on the leading edge surfaces. There could be significant contributions to this carbon coverage from preflight and/or postflight contamination (available controls indicate that most samples have only minor Si preflight contamination). It is also possible that atomic oxygen reactions on the leading edge result in greater volatilization of the carbon component of the deposited silicones, effectively "thinning" the leading edge deposited overlayer.

It was difficult to assess changes in the surface chemical states of these samples because of their tendency to oxidize and hydrate in earth environment. Preflight and postflight surface chemical state could differ from on-flight condition. The flight control samples, including backsides, have accumulated some contamination. This contamination varied significantly in concentration from one control surface to the next, but on average was significantly thinner than on space environment exposed surfaces. Lower contaminant concentrations and higher substrate signals from the flight control surfaces are both consistent with this conclusion. Element signals from the substrate were weak, but were detected on every flight exposed surface where it was possible to differentiate between contaminant film and substrate components. This would be consistent with a contaminant film that has an average thickness of 50 to 100 Å. The contaminant overlayer is probably patchy, with significant areas covered by less than 100 Å, and other areas by greater than 100 Å of molecular film. No pattern of significant difference was noted between substrate signals for leading edge and trailing edge exposed surfaces. Thus, although the Si concentration data suggests greater on-flight deposition of contaminants on the leading edge surfaces, the substrate signal data shows that the XPS data is not conclusive on the relative thicknesses of flight-deposited contamination for leading and trailing edge surfaces.

B. CONTAMINATION ON POLYMER SURFACES

Polymeric materials on LDEF were represented in this study by exposed surfaces of Kapton and fluorinated ethylene (FEP) Teflon from Ag/FEP thermal control blankets. In general, polymer surfaces are clean and reproducible and stable in the earth environment. This simplified postflight analysis of LDEF exposed polymers, and provided a good opportunity to observe carbon contamination and minor contaminants deposited on-flight. Good controls were available for the polymers, and preflight complications were found to be minimal for FEP and Kapton. Changes in the surface chemical state of the polymer surfaces were readily observed. These have been attributed to space environment exposure, though postflight exposures to air may have as-yet undetermined effects on damaged polymer surfaces.

A variety of visible changes were observed in the Ag/FEP surfaces on both leading and trailing edge samples. The exposed leading edge blanket surfaces appeared uniformly foggy or clouded. The exposed

trailing edge blanket FEP surfaces were "patterned" in some areas with alternating transparent and clouded bands. Clouded areas were observed on many blanket edges, particularly near the bends between exposed and masked material ("transition zone"). Areas of orange/brown discoloration were notable near some of the keyhole-shaped vent slots along the edges of the Ag/FEP blankets.

The SEM and XPS results[2] for the exposed Ag/FEP surfaces are summarized in Table 7. The leading edge samples, from row 7 to 11, all had roughened surfaces typical of high velocity atomic oxygen erosion of FEP, as seen in Fig. 1 for FEP exposed on C11 compared to a featureless control surface. The highly textured surfaces gave rise to diffuse light scattering and the consequent cloudy appearance. The XPS data for the control surface showed carbon and fluorine only. The XPS analysis of the exposed surfaces showed that the surface composition of the FEP remaining after the erosion was indistinguishable in carbon and fluorine composition from the control, with trace amounts of some contaminants (Si, N, S, and Cl) and measurable oxygen present. This oxygen could be from the atomic oxygen interaction or from water adsorption from the atmosphere after retrieval. Water adsorption could be enhanced on the erosion-roughened surfaces which have much higher surface area than the control. The surface chemistry of these leading edge samples was identical to clean FEP Teflon, judged by a comparison of the F:C mole ratio and the C1s peak shape. The C1s spectrum from the D7 blanket surface is shown in Fig. 2a; curve-fitting revealed the major CF_2 peak at 292 eV and moderate CF and CF_3 peaks (approximately 10% each) at 289.5 eV and 294 eV, respectively. This matched the spectrum predicted for FEP with an approximate ethylene/propylene comonomer blend of 90%/10% It appeared that deposited contaminants and damaged polymer were both removed during atomic oxygen erosion.

Table 7. Summary of SEM and XPS Results

LDEF Row	SEM Morphology of Exposed FEP Surface	Bay	Surface Si%	Surface O%	C1s Envelope
1	Smooth; particulate contamination	D	0.2	2	Degraded FEP
2		A	0.7	6	Degraded FEP
2		F(Boeing)	2 - 8	11 - 32	Contamination
2	Puckered texture; more distinct in cloudy bands	F(NASA)	8 - 19	30 - 51	Contamination
3 (TE)					
4	Puckered and wrinkled textures in bands	F	0.2 - 7	4 - 31	Contamination
4		A	0.1	3	Degraded FEP
5	Slighty lumpy (B)	B, C,	0.1	3 - 5	Degraded FEP
6	Some areas of puckered texture	C	<0.1	1 - 2	Degraded FEP
7	Eroded, sharp pinnacles (B)	B, D	<0.1	0.6	Clean FEP
8	Eroded, sharp pinnacles	C	<0.1	0.6	Clean FEP
9 (LE)		D, F	0.1 - 0.8	0.8	Clean FEP
10	Eroded, rounded peaks	A	0.1	0.6	Clean FEP
11	Eroded, sharp pinnacles (C)	C,D	<0.1	0.4	Clean FEP
12					
Control FEP	Smooth, featureless		<0.1	<0.1	Clean FEP

Scanning Electron Microscope Image

LDEF TRAY C11 EXPOSED TEFLON

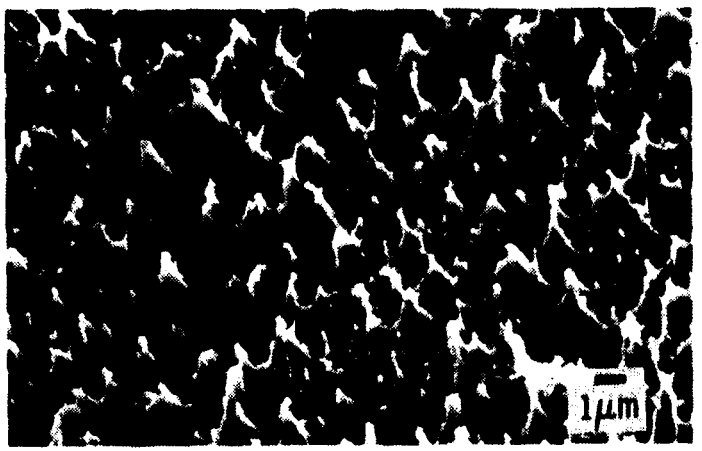

CONTROL TEFLON SURFACE

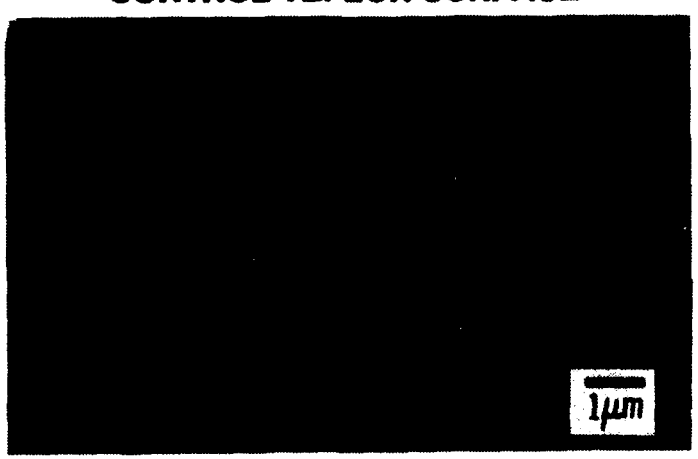

Surface Composition Determined by X-Ray Photoelectron Spectroscopy

MOLE %

C	F	O	OTHER
27	72	0.4	TRACE Si, N, S, Cl
27	73	TRACE	NONE DETECTED

Fig. 1. SEM images and surface composition of FEP. A leading edge surface with atomic oxygen erosion is compared to a featureless control surface.

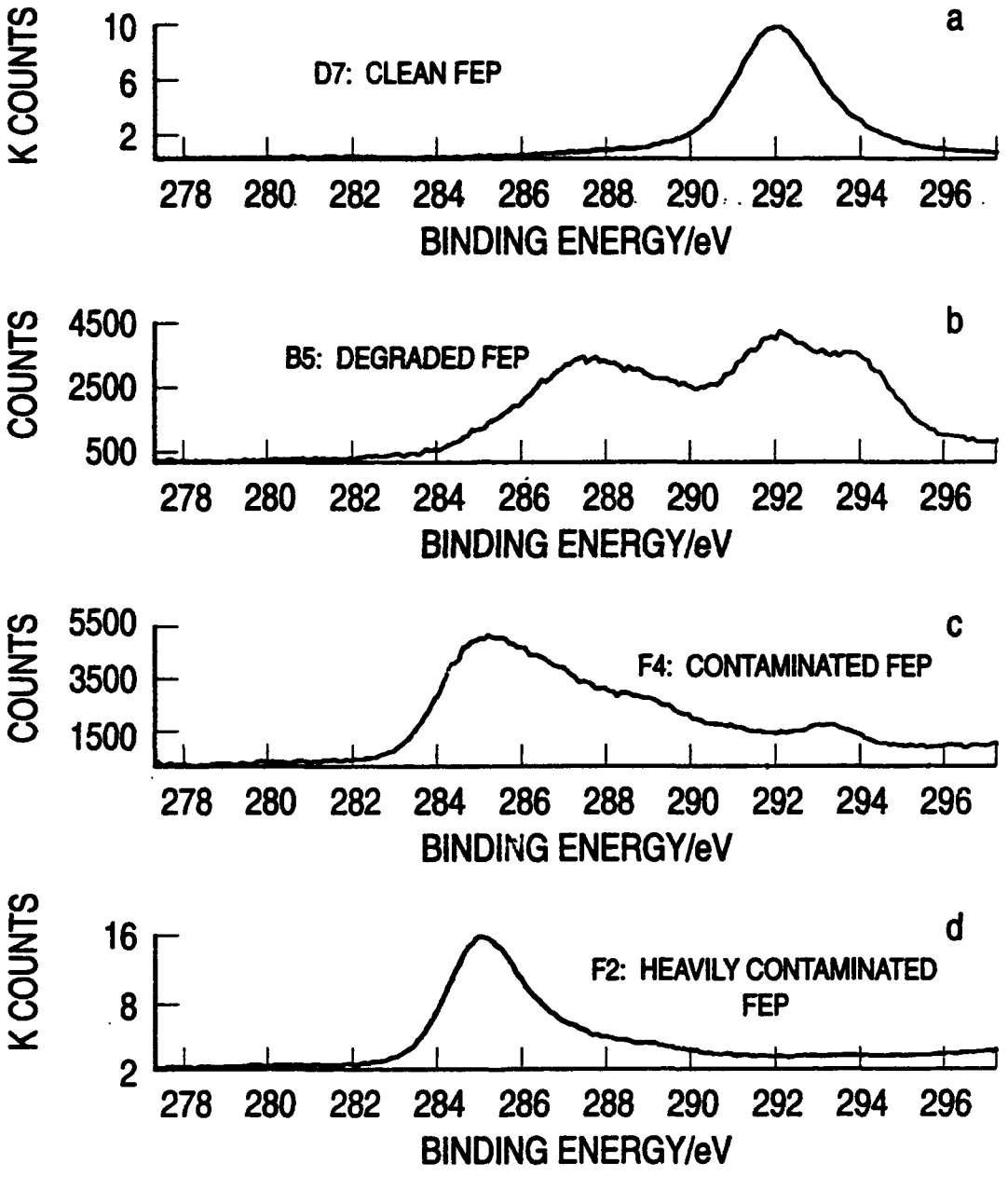

Fig. 2. XPS spectrum of the C1s peak; (a) of the D7 blanket surface representative of clean FEP; (b) of the B5 blanket surface-representative of degraded FEP.; (c) of the F4 blanket surface representative of contaminated FEP; (d) of the F2 blanket surface-representative of heavily contaminated FEP.

The FEP surfaces exposed on the trailing edge of LDEF underwent changes which were observed both by SEM and XPS. The surfaces lost the smooth, featureless texture of the unexposed FEP, even when the amount of contamination remained low, as indicated by low silicon concentration. SEM showed an intriguing variety of new surface textures. Within short distances on some trailing edge samples, both the surface morphology and surface contamination levels were observed to change dramatically, as seen in Fig. 3. The FEP surfaces nearest to the trailing edge row 3 were moderately to heavily contaminated and the blanket surface areas which appear fogged or cloudy on the trailing edge had become sufficiently diffuse to change visibly. The contamination was very nonuniform. It is currently not clear if any causal relationship exists between observed morphology type and surface contamination build-up. It is possible that some morphologies will have a higher probability of trapping or adsorbing outgassed or backscattered species, thereby leading to greater surface contamination buildup. Further from row 3, FEP surfaces showed little texture development and no significant contamination except oxygen, possibly from postflight exposure. It is possible that low atomic oxygen exposure on rows 1, 5, and 6 was sufficient to remove the contaminant overlayer.

XPS data divided the trailing edge surfaces into two categories. The first was characterized by low contamination levels (Si < 1%) and a C1s spectrum, as in Fig. 2b, that differs significantly from that of clean FEP, but does not have a major peak at 285 eV. The second category was characterized by moderate to high levels of surface contamination (Si, O, C, N, and S, and sometimes Cl) and a C1s spectrum dominated by a peak at 285 eV, as seen in Figs. 2c and d. Contaminant carbon was distinguishable from FEP and degraded FEP carbon by binding energy, and was measured at $\leq$ 20% of the total surface composition. The C1s peak at 285 eV is predominantly due to C-C bonds, and is thought to build up on the trailing edge surfaces from decomposition products of outgassed silicones and hydrocarbons. The C1s spectrum in Fig. 2b arises from degradation of the FEP surface, for which the C1s spectrum is shown in Fig. 2a. Curve-fitting shows that the decrease in intensity of the CF_2 peak at 292 eV is accompanied by major increases in intensity at 294 eV, 289.5 eV, and 287 eV, assigned to CF_3, CF, and C-$(CF_n)_4$, respectively. These changes are consistent with damage to the carbon backbone of the Teflon polymer resulting in molecular weight degradation, new chain terminations, branching, and crosslinking through free radical reactions. The solar ultraviolet (UV) radiation exposure of the LDEF surfaces is thought to have caused this FEP surface degradation. The FEP surfaces were also exposed to the stress of about 34,000 thermal cycles, but the maximum temperatures calculated for Ag/FEP blankets on LDEF are less than 0°C and not sufficient to break chemical bonds.[3] Exposure of FEP to the XPS x-ray source for several hours induced similar shifts in the C1s spectrum; almost all of the FEP C1s spectra used for curve-fitting in this study were acquired during the first minute of sample exposure to the x-ray source to minimize surface degradation from the analysis itself. A recent study of the degradation of polytetra-fluoroethylene (PTFE) Teflon by 3 keV electrons showed very similar XPS C1s spectra changes to those seen in Fig. 2b as a function of electron irradiation and subsequent heating to drive off volatiles[4]. Degradation of the PTFE was attributed to the type of damage described above.

The predominant chemical state of Si identified on the trailing edge FEP surfaces was SiO_2. Si concentrations were measured to be $\leq$ 20 mole %, indicating up to about 60% as the oxide. The contaminant film was definitely nonuniform over large areas, and was probably patchy on a submicron scale. Significant areas must be covered by < 100 Å of deposited contamination, because fluorocarbon was detected on each FEP surface analyzed. The damaged FEP layer is probably thicker than the depth of analysis.

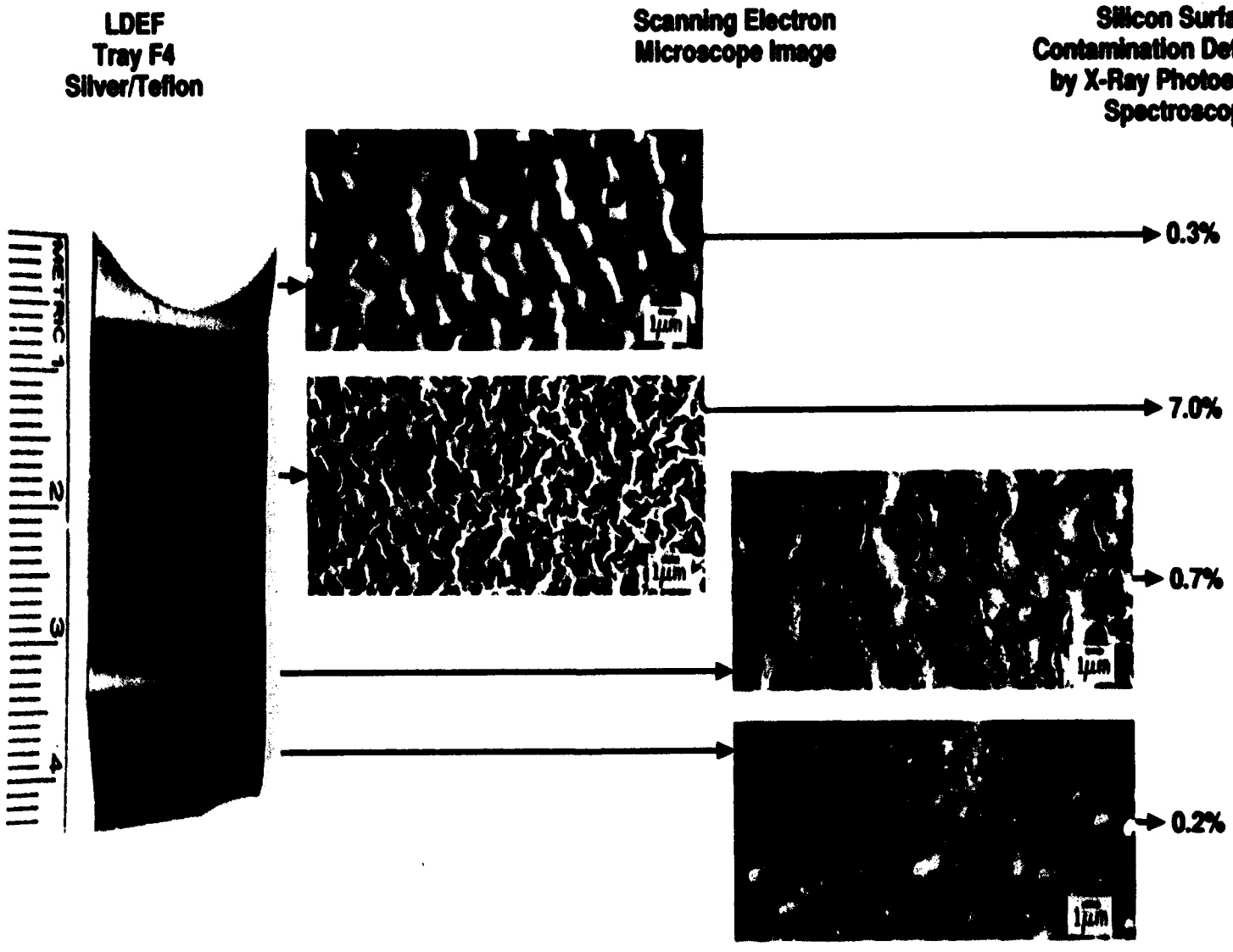

Fig. 3. SEM images of surface morphology changes observed on a section of the trailing edge F4 blanket surface. The FEP surface appeared visibly patterned, as seen in the photograph on the left. The surface contamination, represented by Si concentration, was very nonuniform.

The Ag/FEP thermal control blanket edges were contaminated, in many cases more than the exposed surfaces. Therefore, the masked edges did not provide good flight "control" samples. The transition zone from the exposed surface to the masked edge was particularly prone to contamination build-up. This was probably the result of the combination of high out-gas flux and radiation. The blankets were bent down around the edges of the tray so that the blanket edges were not rigorously shielded from radiation. SEM images from one transition zone, seen in Fig. 4, showed that during atomic oxygen erosion of the FEP surface, undercutting of the contamination and damaged polymer layer played a role in the development of a clean, highly textured surface. Area A, at the periphery of the exposed surface, had a characteristic atomic oxygen erosion pattern. Area D, closer to the blanket edge, was a surface with contamination coverage and UV degraded FEP. Area C, in the center of the transition zone, showed undercutting of the contamination and damaged polymer layer by atomic oxygen erosion. The development of submicron particles of SiO_2 was observed on some edge surfaces by SEM/EDS, as seen in Fig. 5. Such particle development was not detected on any of the other samples included in this study. Areas of orange/brown contamination were observed on some Ag/FEP edge surfaces near keyhole-shaped vent slots in the blanket edges. XPS analysis showed these stains to be high in carbon, sulfur, and nitrogen relative to other contaminated areas. The source of contamination was not identified, but it appears to have contained an amine/amide functionality.

Only two samples of Kapton, from leading edge F9, have been analyzed to date, but the results complemented those for leading edge FEP Teflon. SEM analysis showed the leading edge Kapton had heavy atomic oxygen erosion. Contaminant build-up, as seen in Table 8, was low due to that erosion, totalling < 4 surface mole % excluding oxygen. The observed surface oxygen concentration increases were associated with these contaminants as well as with polymer oxidation. A 5% increase in oxygen-containing surface functionalities was measured by C1s spectrum curve-fitting.

Table 8. XPS Data for Kapton

	Surface Mole %, Normalized								
Kapton Sample	C	O	N	Si	Na	S	K	F	P
Reference	71	21	7.4	0.2	nd	0.1	nd	nd	nd
Exposed #1	62	28	6.8	2	1	0.4	0.3	0.1	tr
Exposed #2	64	27	6.8	1	1	0.3	0.2	0.1	tr

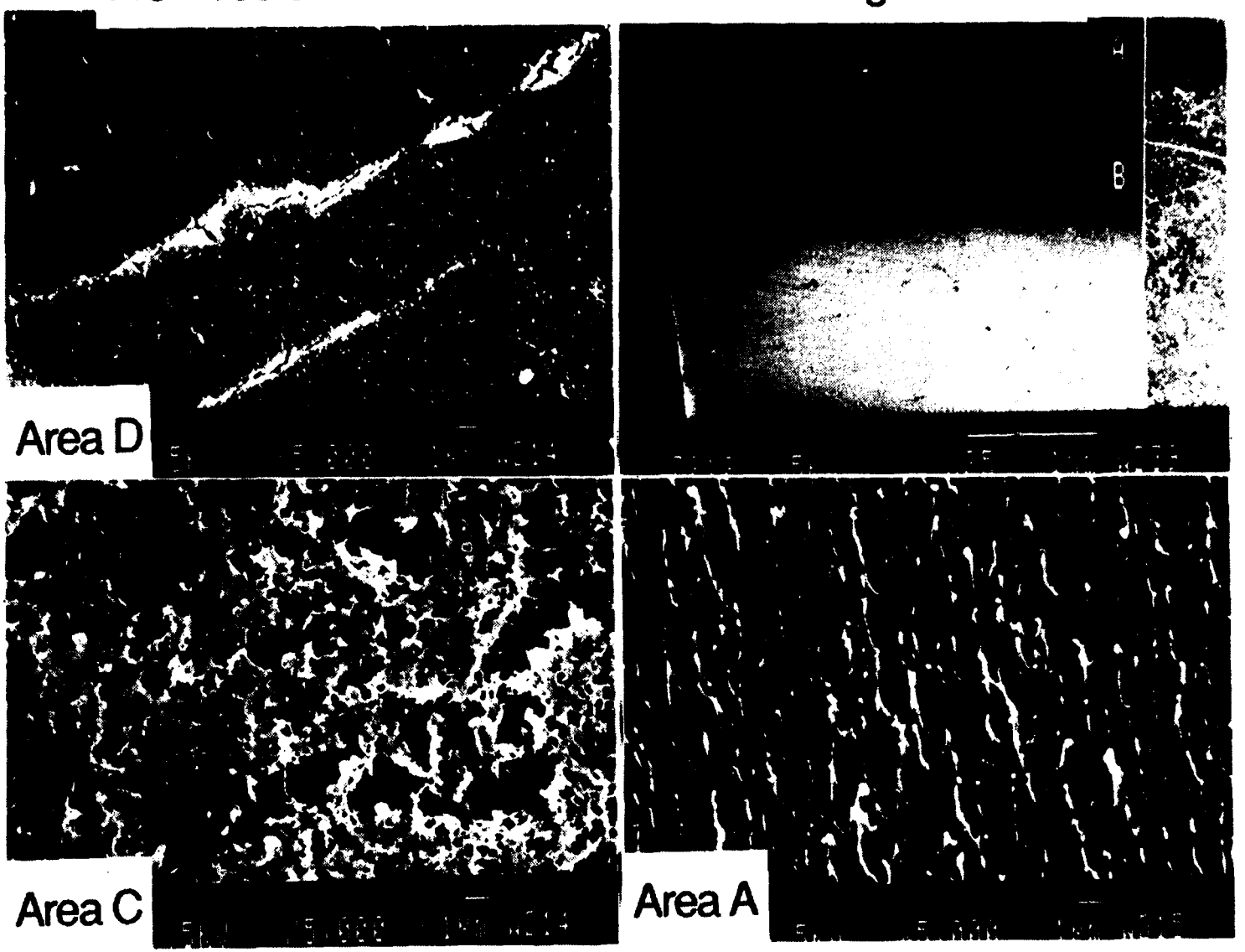

Fig. 4. SEM images of a transition zone on the A10 blanket edge. Area A has the characteristic atomic oxygen erosion pattern. Area D is a surface with contamination coverage and UV degraded FEP. Area C shows undercutting of the contamination and damaged polymer layer.

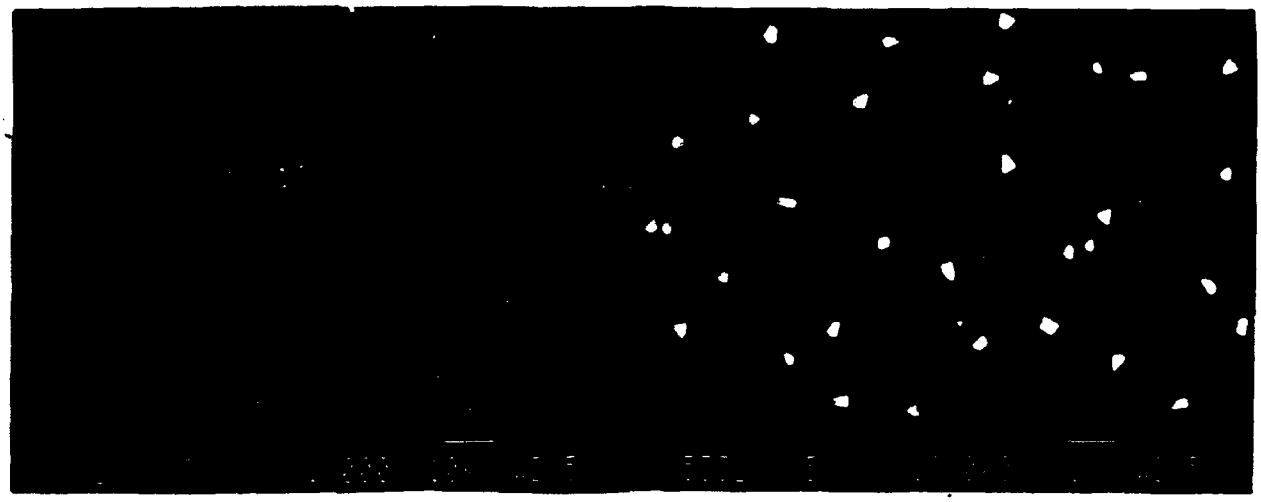

Fig. 5. SEM images of submicron particles of SiO_2 on a masked edge surface of the C8 blanket

IV. SUMMARY

XPS was used to study the average surface composition and chemistry of a variety of LDEF exposed materials. XPS gives excellent surface sensitivity and element detection for contaminant analysis, with minimal sample alteration. SiO_2 and other decomposition products of silicones exposed to the space environment were identified as the predominant surface contaminant for every type and location of material. Deposited carbon residues were distinguishable from preflight contamination on Ag/FEP surfaces. This carbon is thought to come from silicones decomposition and organic contaminants, including the source of the orange/brown stains which had increased carbon, sulfur, and nitrogen concentrations relative to other deposits. Most of the minor (< 1 atom %) and occasionally observed contaminants on the LDEF exposed surfaces were attributed primarily to preflight contamination. This clearly demonstrated the need to maintain good laboratory controls during the study of space environmental effects on materials.

The flight controls (no direct line of sight to the space environment) were found to have accumulated some contamination, but generally less than exposed surfaces. The polymeric materials studied had low contamination on the leading edge surfaces due to atomic oxygen erosion. All other materials had higher average Si contamination on leading edge than on trailing edge surfaces, probably due to the return flux associated with atmospheric backscatter. For individual pairs of samples, measured Si concentration leading edge/trailing edge ratios varied from 0.4 to 15, with a median of about 1.5 and an average of about 4. Element signals from some substrates were weak, but were detected on every flight exposed surface where it was possible to differentiate between contaminant film and substrate components. This would be consistent with a contaminant film that has an average thickness of 50 to 100 Å. The contaminant overlayer is probably patchy, with significant areas covered by less than 100 Å, and other areas by greater than 100 Å of molecular film. No pattern of significant difference was noted between the intensity of substrate signals for leading edge and trailing edge exposed surfaces. Thus, although the Si concentration data suggested greater on-flight deposition of contaminants on the leading edge surfaces, the XPS analysis was not conclusive on the relative total thicknesses of flight-deposited contamination for leading and trailing edge surfaces.

REFERENCES

1. Mallon, J. J., Uht, J. C., and Hemminger, C. S., "Surface Analyses of Composites Exposed to the Space Environment on LDEF." Submitted for publication, 1991.

2. Hemminger, C. S., Stuckey, W. K., and Uht, J. C., "Space Environmental Effects on Silvered Teflon Thermal Control Surfaces." *First LDEF Post-Retrieval Symposium*, June 1991. See also NASA CP 3134, 1992.

3. Berrios, W. M. and Sampair, T. R., "LDEF Post Flight Thermal Analysis." LDEF Science Office, NASA Langley Research Center.

4. Wheeler, D. R. and Pepper, S. V., "X-ray Photoelectron and Mass Spectroscopic Study of Electron Irradiation and Thermal Stability of Polytetrafluoroethylene." *J. Vac. Sci. Technol.* Vol A8, No. 6, Nov/Dec 1990, pp. 4046-4056.

TECHNOLOGY OPERATIONS

The Aerospace Corporation functions as an "architect-engineer" for national security programs, specializing in advanced military space systems. The Corporation's Technology Operations supports the effective and timely development and operation of national security systems through scientific research and the application of advanced technology. Vital to the success of the Corporation is the technical staff's wide-ranging expertise and its ability to stay abreast of new technological developments and program support issues associated with rapidly evolving space systems. Contributing capabilities are provided by these individual Technology Centers:

Electronics Technology Center: Microelectronics, solid-state device physics, VLSI reliability, compound semiconductors, radiation hardening, data storage technologies, infrared detector devices and testing; electro-optics, quantum electronics, solid-state lasers, optical propagation and communications; cw and pulsed chemical laser development, optical resonators, beam control, atmospheric propagation, and laser effects and countermeasures; atomic frequency standards, applied laser spectroscopy, laser chemistry, laser optoelectronics, phase conjugation and coherent imaging, solar cell physics, battery electrochemistry, battery testing and evaluation.

Mechanics and Materials Technology Center: Evaluation and characterization of new materials: metals, alloys, ceramics, polymers and their composites, and new forms of carbon; development and analysis of thin films and deposition techniques; nondestructive evaluation, component failure analysis and reliability; fracture mechanics and stress corrosion; development and evaluation of hardened components; analysis and evaluation of materials at cryogenic and elevated temperatures; launch vehicle and reentry fluid mechanics, heat transfer and flight dynamics; chemical and electric propulsion; spacecraft structural mechanics, spacecraft survivability and vulnerability assessment; contamination, thermal and structural control; high temperature thermomechanics, gas kinetics and radiation; lubrication and surface phenomena.

Space and Environment Technology Center: Magnetospheric, auroral and cosmic ray physics, wave-particle interactions, magnetospheric plasma waves; atmospheric and ionospheric physics, density and composition of the upper atmosphere, remote sensing using atmospheric radiation; solar physics, infrared astronomy, infrared signature analysis; effects of solar activity, magnetic storms and nuclear explosions on the earth's atmosphere, ionosphere and magnetosphere; effects of electromagnetic and particulate radiations on space systems; space instrumentation; propellant chemistry, chemical dynamics, environmental chemistry, trace detection; atmospheric chemical reactions, atmospheric optics, light scattering, state-specific chemical reactions and radiative signatures of missile plumes, and sensor out-of-field-of-view rejection.